MAUSAM, **77**, 3 (July 2026), 961-974

MAUSAM

DOI: https://doi.org/10.54302/mausam.v77i3.7172
Homepage: https://mausamjournal.imd.gov.in/index.php/MAUSAM

UDC No.550.831:551.24:550.36

Geological structure identification and derivative analysis method with lithological inverse modelling in Mount Gede-Pangrango geothermal prospect area using gravity data

AGUS SETYAWAN[1*], PUTRI PERMATA HATI SURYO BASUKI[2], AHMAD ALI MUCKHAROM[3], TONY YULIANTO[1], RAHMAT GERNOWO[1], UDI HARMOKO[1] and MUHAMMAD FAHMI[1]

[1]*Department of Physics, Faculty of Science and Mathematics, Diponegoro University, Semarang, Indonesia*

[2]*Undergraduate Student, Department of Physics, Faculty of Science and Mathematics, Diponegoro University, Semarang, Indonesia*

[3]*Graduate Student, Department of Physics, Faculty of Science and Mathematics, Diponegoro University, Semarang, Indonesia*

(*Received 26 June 2025, Accepted 1 December 2025*)

***Corresponding author's email: agussetyawan@fisika.fsm.undip.ac.id**

सार – प्रशांत महासागर के 'रिंग ऑफ फायर' के साथ स्थित पश्चिम जावा में गेडे-पंगरांगो ज्वालामुखी परिसर की भू-तापीय संभावनाएं महत्वपूर्ण क्षमता प्रदर्शित करती हैं, जो सोल्फतारास (Solfataras), फ्यूमरोल्स (Fumaroles) और गर्म झरनों जैसे सतही अभिव्यक्तियों द्वारा इंगित की जाती हैं। पिछले अध्ययनों ने 2000-2800 मीटर की गहराई पर क्वाटरनरी ज्वालामुखीय चट्टानों के भीतर एक उच्च तापमान वाले जलाशय (290-300°C) की उपस्थिति की सूचना दी है; हालांकि, भू-तापीय प्रणाली को नियंत्रित करने वाली उपसतह संरचनाओं और भ्रंशों (Faults) के संबंध में अनिश्चितताएं बनी हुई हैं। यह अध्ययन इन विशेषताओं की जांच करने के लिए सैटेलाइट-व्युत्पन्न गुरुत्वाकर्षण डेटा (GGMPlus) और ऊंचाई डेटा (ERTM) को नियोजित करता है। भू-तापीय गतिविधि से जुड़ी उपसतह संरचनाओं को रेखांकित करने के लिए फर्स्ट हॉरिजॉन्टल डेरिवेटिव (FHD) और सेकेंड वर्टिकल डेरिवेटिव (SVD) सहित एज-डिटेक्शन फिल्टर लागू किए गए थे। अवशिष्ट विसंगति मानचित्र (Residual anomaly map) तीन प्राथमिक क्षेत्रों को प्रकट करता है: उच्च, मध्यम और निम्न विसंगतियां। उच्च विसंगतियां माउंट गेडे और माउंट पंगरांगो के आसपास केंद्रित हैं, जो घनी ज्वालामुखीय चट्टानों या उथले अंतर्भेदन (Shallow intrusions) को दर्शाती हैं, जबकि कम विसंगतियां पायरोक्लास्टिक जमाव और हाइड्रोथर्मली परिवर्तित चट्टानों के अनुरूप हैं। FHD और SVD विश्लेषण उत्तर पूर्व-दक्षिण पश्चिम (NE-SW) की ओर झुके हुए भ्रंशों को उजागर करते हैं जो भू-तापीय द्रव प्रवासन के लिए प्राथमिक मार्गों के रूप में कार्य करते हैं, जिसकी पुष्टि गर्म झरनों और कवाह रातु क्रेटर के साथ फ्रैक्चर के संरेखण द्वारा होती है। 2D क्रॉस-सेक्शनल मॉडल एक प्रमुख भ्रंश द्वारा नियंत्रित 1-2 किमी की गहराई पर एक कम घनत्व वाले जलाशय को इंगित करता है, जिसके नीचे अंतर्भेदी चट्टानें ऊष्मा स्रोत के रूप में कार्य करती हैं। इसके अलावा, 3D घनत्व मॉडलिंग माउंट गेडे और माउंट पंगरांगो के बीच एक जुड़ी हुई भू-तापीय प्रणाली को प्रदर्शित करती है, जो दोनों ज्वालामुखियों के नीचे उच्च-पारगम्यता वाले क्षेत्रों (High-permeability zones) द्वारा अभिलक्षित है।

ABSTRACT. The geothermal prospects of the Gede–Pangrango volcano complex in West Java, situated along the Pacific Ring of Fire, exhibit significant potential indicated by surface manifestations such as solfataras, fumaroles, and hot springs. Previous studies have reported the presence of a high-temperature reservoir (290–300°C) within Quaternary volcanic rocks at depths of 2000–2800 meters; however, uncertainties remain regarding the subsurface structures and faults that control the geothermal system. This study employs satellite-derived gravity data (GGMPlus) and elevation data (ERTM) to investigate these features. Edge-detection filters, including the First Horizontal Derivative (FHD) and Second Vertical Derivative (SVD), were applied to delineate subsurface structures associated with geothermal activity. The residual anomaly map reveals three primary zones: high, moderate, and low anomalies. High anomalies are concentrated around Mount Gede and Mount Pangrango, reflecting dense volcanic rocks or shallow intrusions, whereas low anomalies correspond to pyroclastic deposits and hydrothermally altered rocks. FHD and SVD analyses highlight northeast–southwest (NE–SW) trending faults that serve as primary pathways for geothermal fluid migration, confirmed by the alignment of fractures with hot springs and the Kawah Ratu crater. The 2D cross-sectional model indicates a low-density reservoir at

depths of 1–2 km controlled by a major fault, underlain by intrusive rocks acting as the heat source. Furthermore, the 3D density modeling demonstrates a connected geothermal system between Mount Gede and Mount Pangrango, characterized by high-permeability zones beneath both volcanoes.

Key words – GGMPlus, Derivative analysis, Gravity method, Mount Gede-Pangrango, Density.

1. Introduction

West Java is one of the regions in Indonesia with significant geothermal potential due to its position along the Pacific Ring of Fire. One of the most important prospects is located in the Mount Gede and Mount Pangrango area. Geothermal manifestations in this region include solfataras and fumaroles in the Ratu Crater, as well as hot springs in Cipanas. The solfataras and fumaroles exhibit temperatures ranging from 81 °C to 167 °C, while the Cipanas hot springs reach around 35°C with a neutral pH and a distinctive H_2S odor (KESDM, 2017). The geothermal reservoir is characterized by high temperatures of about 290–300 °C, hosted in Quaternary volcanic rocks at a depth of approximately 2000 meters (Iswahyudi, 2014).

Geothermal exploration in the Mount Gede–Pangrango region, particularly around Cipanas, has been conducted for several decades to investigate the geothermal system and its resource potential (Gunawan *et al*., 2022; Haty *et al*., 2023). In 2023, PT Daya Mas Geopatra Pangrango, a subsidiary of the Sinarmas Group, was assigned a Preliminary Survey and Exploration (PSPE) with a resource target of 85 MW and a development plan for a 55 MW geothermal power plant (PLTP), which is expected to begin commercial operation in 2030 (KESDM, 2023). The exploration program applies directional drilling technology to reach geothermal reservoirs in steep terrain with slopes of up to 60 degrees, while maintaining the ecological sustainability of Mount Gede - Pangrango National Park. These drilling activities have provided greater insights into the geothermal reservoir characteristics, which are hosted in pyroclastic deposits to depths exceeding 2800 meters, with a heat source derived from andesitic magma intrusions.

In addition to drilling, geophysical methods have also been applied, including land surface temperature (LST) mapping using satellite imagery, as well as physical and chemical analysis of hot spring waters as indicators of geothermal system activity (Indriana *et al*., 2026; Pratiwi *et al*., 2026). These approaches provide valuable information on geothermal distribution and the possible presence of subsurface reservoirs (Agustin, 2019; Haty *et al*., 2023). By integrating geological exploration, drilling, and geophysical investigations, the development of the Cipanas geothermal power plant is expected to make a significant contribution to renewable and sustainable energy supply in West Java.

Despite being more extensively studied than many other geothermal prospects in Indonesia, the Mount Gede–Pangrango region still faces uncertainties regarding the subsurface structures that control the geothermal system. In particular, it remains unclear whether the two volcanoes are interconnected as a single integrated geothermal system or if they function independently. Furthermore, the boundaries and extent of the geothermal resource have not yet been clearly defined, thus requiring further investigation to improve understanding of the structural framework and the overall geothermal potential.

This study aims to address these uncertainties by analyzing gravity data to delineate geological structures in the manifestation zone and to evaluate whether the Mount Gede and Mount Pangrango geothermal systems are interconnected. The results are expected to provide a basis for determining test drilling locations and identifying promising areas for further exploration.

2. Data and methodology

2.1. *Geological setting*

The general geological background of the study area was incorporated at both the qualitative and quantitative stages of the interpretation of the Bouguer gravity anomaly. A clear understanding of the regional geology of Bogor and its surrounding areas is required for the interpretation of the gravity data. The red triangles indicate the location of the two mountains (Mount Pangrango and Mount Gede) (see Fig. 1).

The highest topographic elevations are represented by red to purple colors and are concentrated in the central mountainous area of both volcanoes, ranging from 2,098.4 meters to 2,992 meters. Meanwhile, the medium topographic elevations are shown in green to orange, with heights between 1,260.5 meters and 2,098.3 meters. The surrounding lowland areas are indicated by dark to light blue colors, representing the foothills of Mount Gede–Pangrango, with elevations ranging from 806 meters to 1,260.4 meters.

The stratigraphic sequence of rock units in the Mount Gede–Pangrango research area (see Fig. 2), from oldest to youngest, consists of the volcanic deposits of Mount Masigit (Qovm), the pyroclastic flow of Pangrango (Paap), the lava flow of Pangrango (Paal), the pyroclastic fall of Pangrango (Pajp), the lava flow of Pasirpogor from Gede Crater (Ppal), the lava flow of Gumuruh from Gede

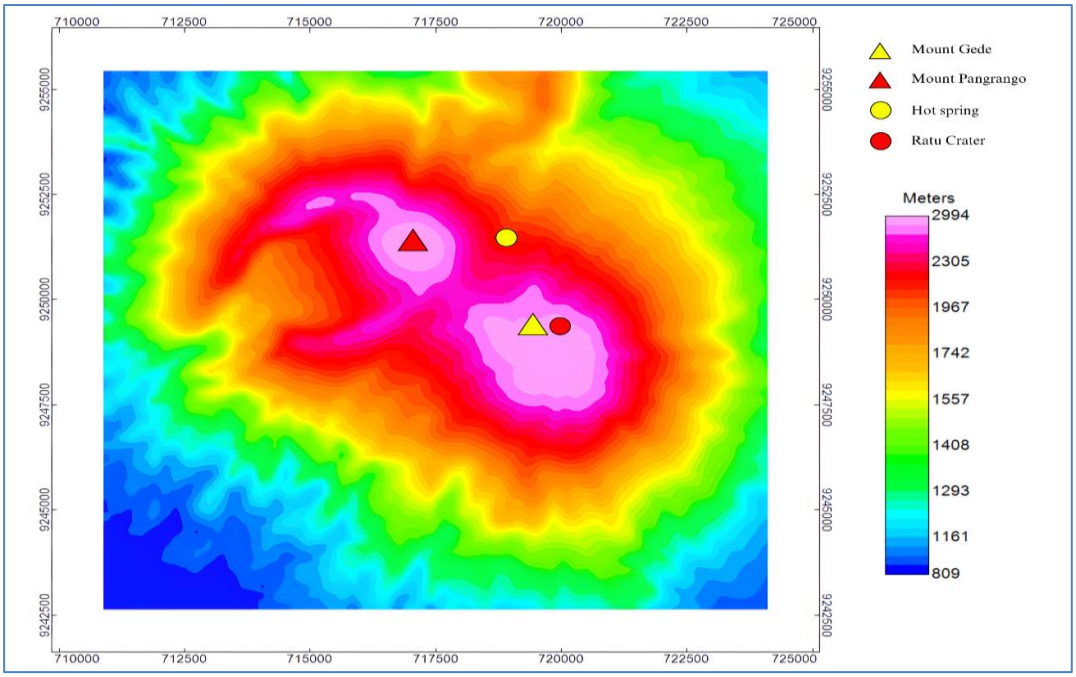

Fig. 1. Elevation map showing the location of Mount Gede-Pangrango and geothermal manifestations

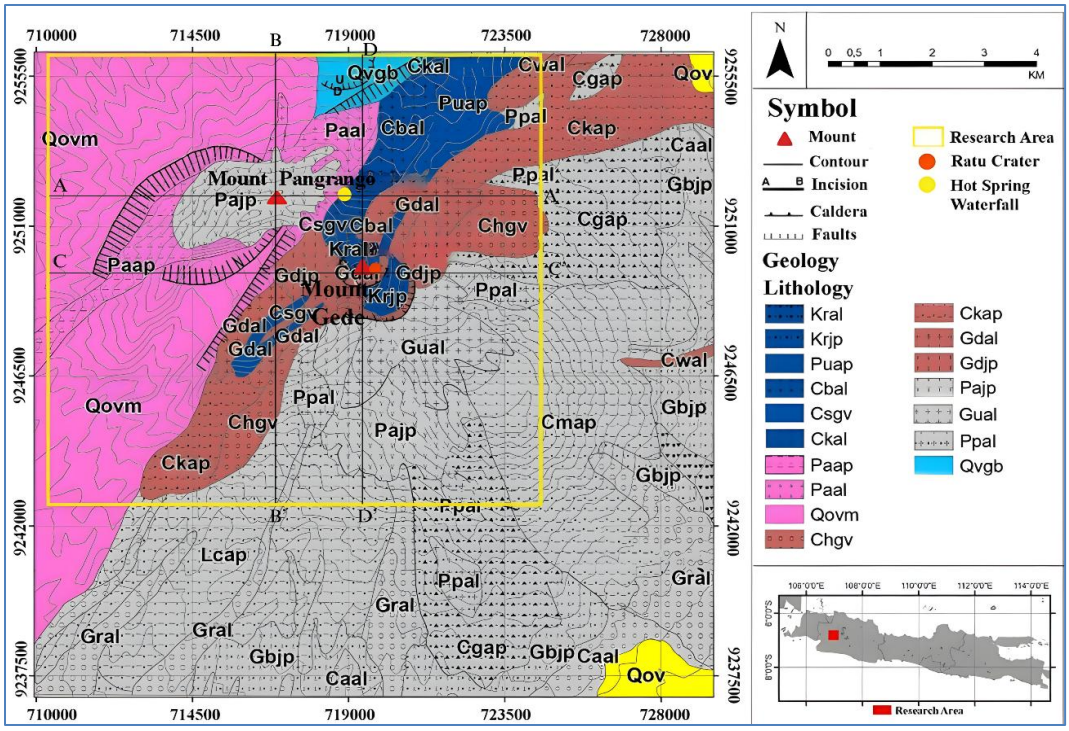

Fig. 2. Surface geology map of the study area, modified from previous work done by Situmorang & Hadisantono, (1992)

Crater (Gual), the volcanic eruption of Ciherang from Gede Crater (Chgv), the pyroclastic flow of Cikundul (Ckap), the pyroclastic fall of Gede from Gede Crater (Gdjp), the lava flow of Gede from Gede Crater (Gdal), the pyroclastic flow of Putri from Ratu Crater (Puap), the lava flow of Cibodas from Ratu Crater (Cbal), the lahar flow of Cikidul (Ckal), the volcanic eruption of Cisaat from Ratu Crater (Csgv), the lava flow of Ratu Crater (Kral), the pyroclastic fall from Ratu Crater (Krjp), and the volcanic deposits of Gegerbentang (Qvgb).

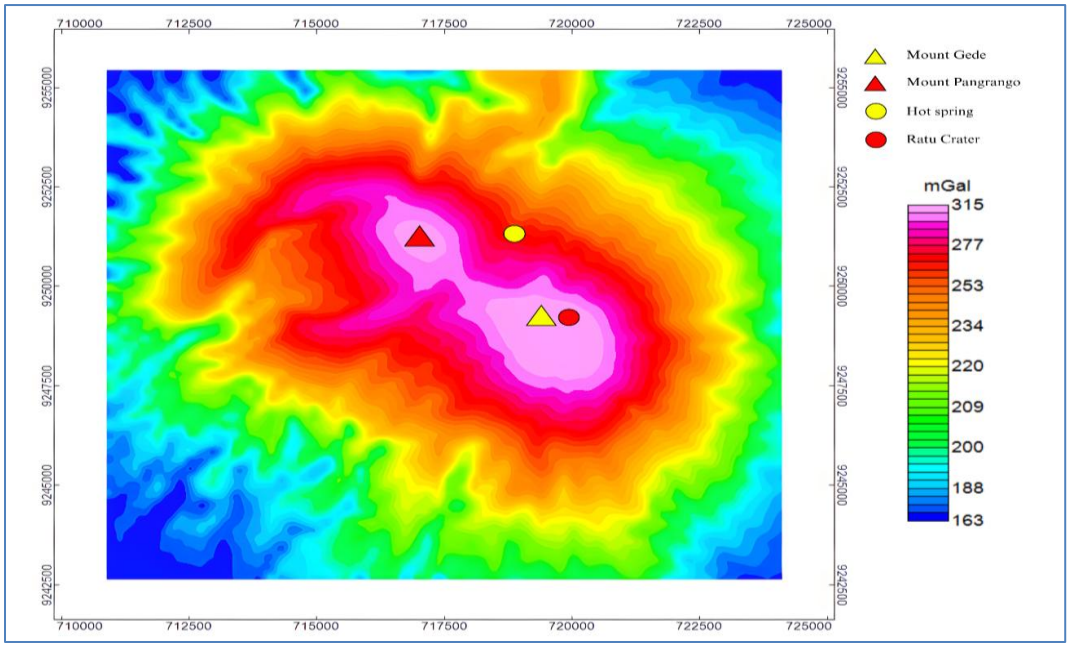

Fig. 3. Free air anomaly map of the study area

Structurally, the research area is controlled by fault systems trending northeast–southwest (NE–SW) and north–south (N–S), which influence the lithological development and eruption patterns. The presence of the Pangrango caldera is indicated by the caldera boundary symbol on the map, formed as a result of major explosive eruptions in the past. Meanwhile, the Ratu Crater of Mount Gede serves as the center of post-caldera eruptions, with the distribution of pyroclastic, lava, and lahar deposits controlled by ring fractures of the caldera and local faults. Geothermal manifestations in the area are indicated by the occurrence of hot springs located on the slopes of Mount Pangrango and Mount Gede. These manifestations strengthen the indication that magmatic activity is still present beneath the surface, providing evidence of significant geothermal energy potential in the Gede–Pangrango region.

2.2. *Methods*

The gravity method is one of the passive methods, meaning that it does not damage the environment. The gravity method measures variations in the Earth's gravitational field caused by differences in mass density or density between rocks below the rock surface. This method applies the principle of Newton's law of gravity to two objects (Blakely, 1995; Telford *et al*., 1990). Preliminary exploration studies can use gravity methods to provide information about the research area such as rock density, geothermal sources, and subsurface structures. Geological structures are rock formations resulting from geological processes and deformations such as folds, faults, and fractures. Faulting is a form of deformation caused by excessive forces acting on rocks (Agustine *et al*., 2023; Hafidh *et al*., 2025; Indriana *et al*., 2021; Prihatini *et al*., 2025; Setyawan *et al*., 2015). The gravity method using GGMplus satellite data can be an alternative solution with lower costs and a wider area (Hirt *et al*., 2013). The GGMPlus data obtained is still influenced by several external gravity fields such as valleys or mountains around the research area, so corrections are needed for data measurement. The data correction used, free air correction (FAC) to reduce the effect of altitude variation with the aim of obtaining the free air anomaly (FAA) (see Fig. 3) (Reynolds, 1997), terrain correction (TC) to reduce the effect of topographic variations on the earth's surface at the same altitude (Lowrie, 2007), and Bouguer correction (BC) to minimize the effect of mass between the measurement point and the center of the earth (Tatham, 2011).

$$CBA = FAA - BC + TC \quad (1)$$

After the gravity corrections were applied, an anomalous value known as the Complete Bouguer Anomaly (CBA) was obtained (Fig. 4). The CBA is the difference between the measured gravity value and the theoretical earth gravity at a given observation point (Blakely, 1995). This value indicates the variation in mass density within an area. The CBA incorporates regional and residual anomalies that are associated with variations in rock mass density. The upward continuation method is applied to distinguish between regional and residual anomalies.

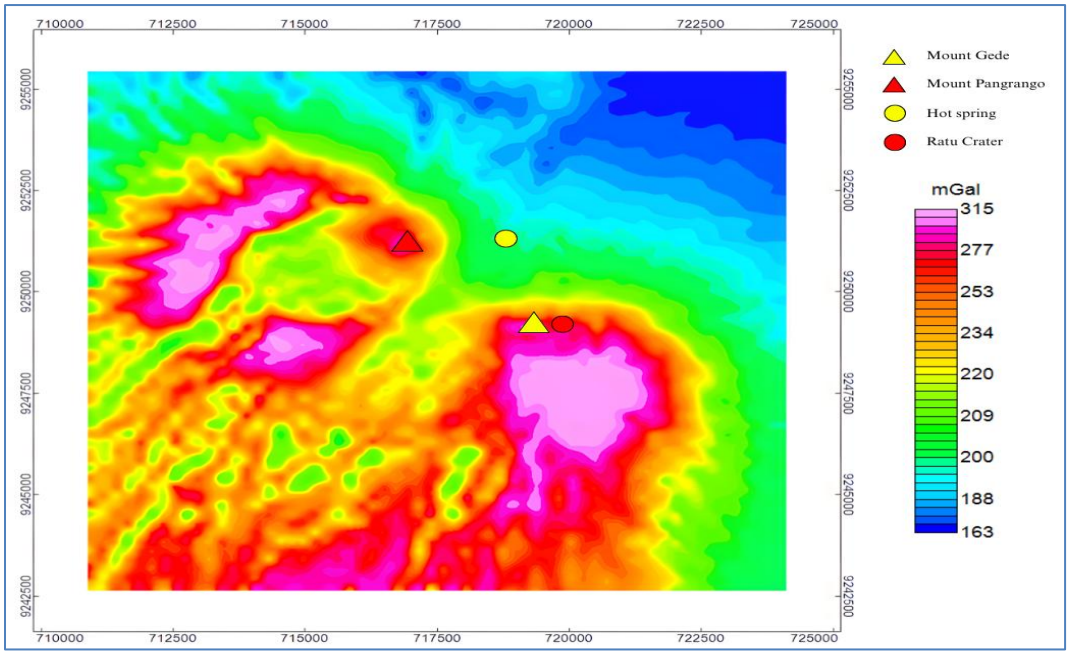

Fig. 4. Complete Bouguer anomaly map of Mount Gede-Pangrango Geothermal prospect area (ρ = 2.1739 g/cm^3)

Derivative analysis can be used to determine the boundaries of anomalies where faults are suspected. The derivation is performed using the First Horizontal Derivative (FHD) (Hinze *et al*., 2012).

$$FHD = \sqrt{(\frac{\partial g}{\partial x})^2 + (\frac{\partial g}{\partial y})^2} \quad (2)$$

In FHD analysis, the maximum value (peak) represents the presence of a fault structure (Setyawan *et al*., 2015). Meanwhile, in SVD analysis, fault structure is represented by the zero value. The SVD equation results from deriving the Laplace equation (Yasmin *et al*., 2024).

$$\nabla^2 \Delta g = 0 \quad (3)$$

$$\frac{\delta^2 \Delta g}{\delta x^2} + \frac{\delta^2 \Delta g}{\delta y^2} + \frac{\delta^2 \Delta g}{\delta z^2} = 0 \quad (4)$$

The equation for the second vertical derivative is in accordance with the equation 5 below:

$$\frac{\delta^2 \Delta g}{\delta z^2} = -\left(\frac{\delta^2 \Delta g}{\delta x^2} + \frac{\delta^2 \Delta g}{\delta y^2}\right) \quad (5)$$

The Equation (5) can be expressed as Eq. (6) (Sarkowi, 2014):

$$\frac{\delta^2 \Delta g}{\delta z^2} = -\left(\frac{\delta^2 \Delta g}{\delta x^2}\right) \quad (6)$$

Based on the equation above, the second vertical derivative anomaly $\left(\frac{\delta^2 \Delta g}{\delta z^2}\right)$ can be calculated from the first derivative of the first horizontal derivative.

$$\left(-\frac{\delta}{\delta x}\left(\frac{\delta \Delta g}{\delta x}\right)\right) \quad (7)$$

In inversion modeling, model parameters are derived directly from observational data, which creates a direct approach to understanding the properties of the Earth's subsurface. A match between the inversion calculations produced in modeling a representative subsurface and the observed data. Variations in the subsurface model result from the match. The presence or absence of data, errors during data acquisition and the characteristics of the phenomenon being studied greatly affect this (Muttaqien & Nerjaman, 2021; Setyawan *et al*., 2024).

The inversion modeling was carried out using the Voxel Modeling Tool from Horin Geophysical Exploration software. By using residual anomalies, researchers can be more accurate and more focused on local characteristics related to geothermal potential and see the presence of subsurface structures.

3. Results and discussion

The research uses secondary data in the form of GGMplus satellite data, Free Air Anomaly (FAA) and elevation. The geographical position of the research area is 724054.84 to 710957.12 and 9242692.16 to 9255354.65

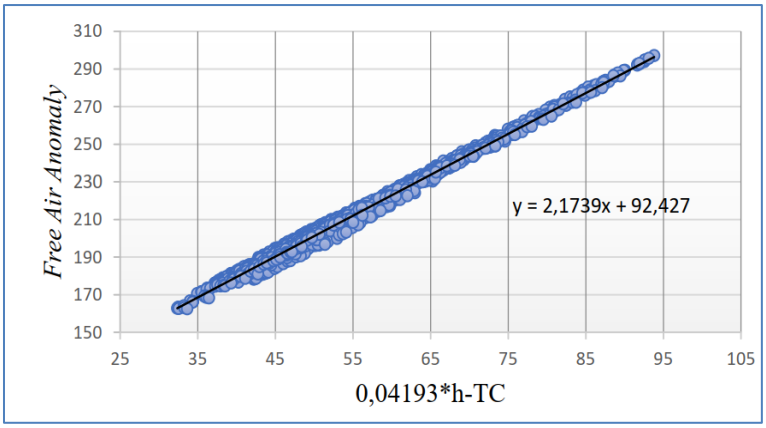

Fig. 5. Parasnis graph of the study area (Parasnis & Cook, 1952)

which is included in the UTM 48˚S zone. The dataset comprises 3,480 data points. The obtained secondary data need to go through several stages to be analyzed. The stages carried out are Bouguer correction and terrain correction. The result obtained from the correction is the Bouguer anomaly value. Furthermore, further data processing is carried out by performing upward continuation and also derivative analysis, and inverse modelling with Horin Geophysical Exploration Software.

Mount Gede-Pangrango as the research area is located on the island of Java in West Java Province. The topography of the research area describes the low and high surface of the earth. Topographic contour map using Horin Geophysical Exploration. The research area has an altitude of 809 m to 2994 m above sea level (Fig. 1).

The GGMPlus data was extracted to produce a contour map of the Free Air Anomaly. During gravity data processing using GGMPlus, the Free Air Anomaly values were corrected for the free-air effect. FAA values in the study area range from 163 to 315 mGal, with the highest values located over Mount Gede-Pangrango, marked in pink. Theoretically, the Free Air Anomaly is proportional to topographic elevation, as described by the equation $gFAA = 0.3086h$ (Telford *et al*., 1990).

To estimate the average rock density in the study area, the Parasnis method was used (Fig. 5). This method involves creating a linear regression plot based on the Parasnis equation, which expresses the relationship between the Free Air Anomaly and the Bouguer correction without the influence of density, and then subtracting the field correction value (Parasnis, 1997; Saxena & Candela, 1986). The average density is determined from the slope of the regression line. As shown in Fig. 5, the average rock density in the study area is 2.17 g/cm^3. This value aligns with local geological data indicating that the area is dominated by basic igneous rocks with a density range of 2.09 to 3.17 g/cm^3 and an average of 2.79 g/cm^3 (Kusumadinata, 1979).

Complete Bouguer Anomaly (CBA) (Fig. 4) is obtained after applying the Bouguer and terrain corrections. CBA values range from 71.94 to 101.69 mGal. Bouguer anomalies are a combination of regional and residual anomalies. Therefore, separation is needed using the upward continuation method to distinguish shallow and deep anomaly sources. The upward continuation process was performed using Horin Geophysical Exploration to obtain the regional anomaly (Telford *et al*., 1990). The residual anomaly was then obtained by subtracting the regional anomaly values from the Bouguer anomaly. In this study, the regional anomaly was calculated at an elevation of 4000 meters, as shallow anomalies are no longer apparent at this height. The distribution of regional anomaly values is not significantly different from the Bouguer anomaly, as the dominant influence comes from shallow residual anomalies (Fig. 6). Meanwhile, Fig. 7 displays the residual anomaly map, which shows more complex anomaly patterns due to variations in the density contrast of shallower rock formations (Blakely, 1995; Telford *et al*., 1990).

A study by Gunawan *et al*. (2022) also performed residual anomaly separation using the Butterworth filter method, and the results show consistency with the upward continuation method used in this study. These findings confirm that high anomalies are concentrated over the Mount Gede-Pangrango massif, in line with the results of this research.

According to Blakely (1995), the first-order horizontal derivative (Fig. 8) is employed to identify lateral density variations in residual anomalies. In edge detection methods, this derivative is particularly useful as

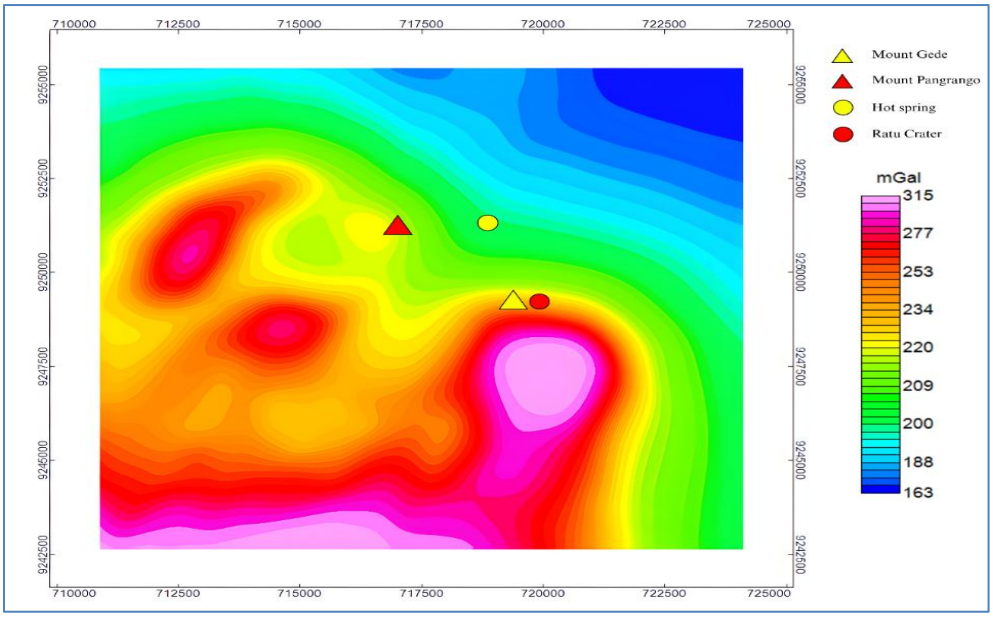

Fig. 6. Upward Continuation from 4000 meters

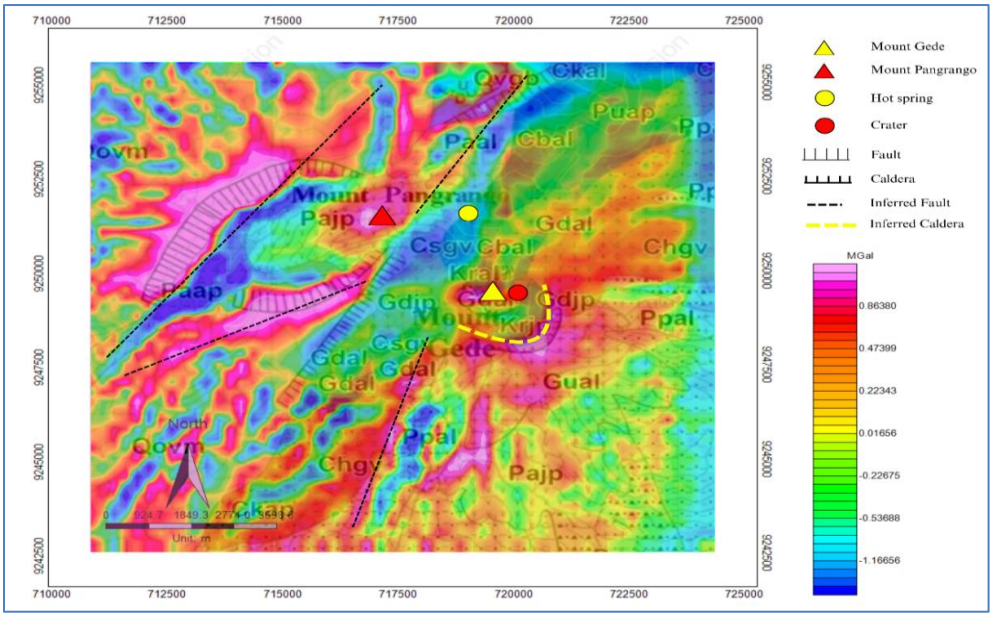

Fig. 7. Residual map of the Mount Gede-Pangrango Geothermal Area

it requires the computation of two first-order horizontal derivatives of the field, although it is sensitive to noise (Phillips, 2002). This filtering technique is considered effective because shallow sources typically generate gravity anomalies in which the horizontal gradient reaches its maximum over the edges or boundaries (Eyike *et al*., 2010; Muckharom *et al*., 2026). The horizontal derivative is therefore applied to delineate the boundaries of broad anomaly sources, since it yields peak values where abrupt gravity changes occur, as expressed in Eq. (2).

Derivative analysis is an interpretation technique that utilizes derivative or Laplacian derivatives along the x, y, and z axes. This method includes four types: first horizontal derivative, second horizontal derivative, first vertical derivative, and second vertical derivative

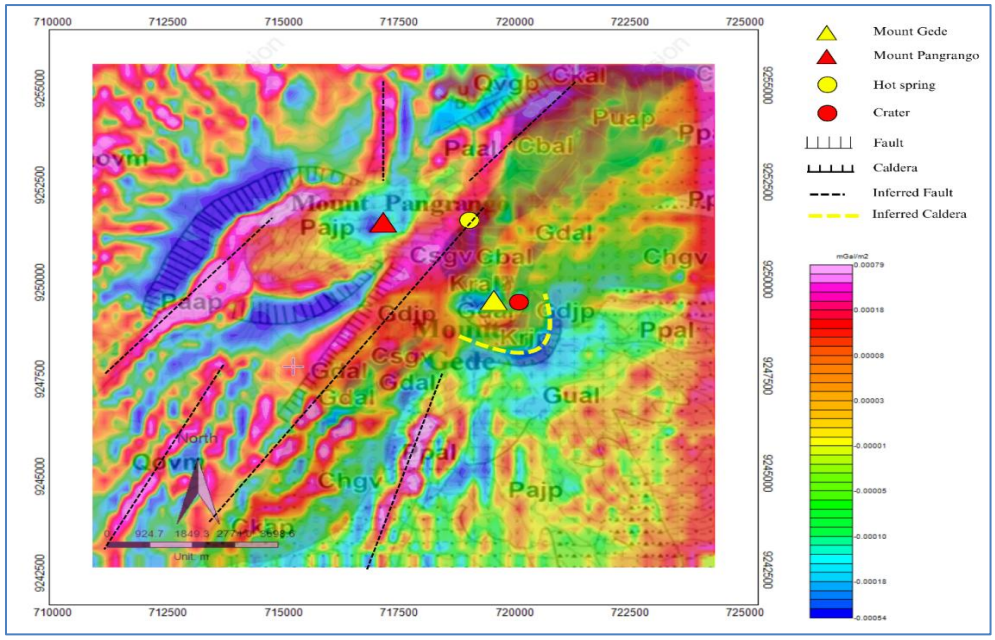

Fig. 8. Horizontal derivative representation of Mount Gede-Pangrango Geothermal Prospect area. The high-value zones indicated in red and purple are the possible contact zones. The dotted black lines are the inferred faults in the field

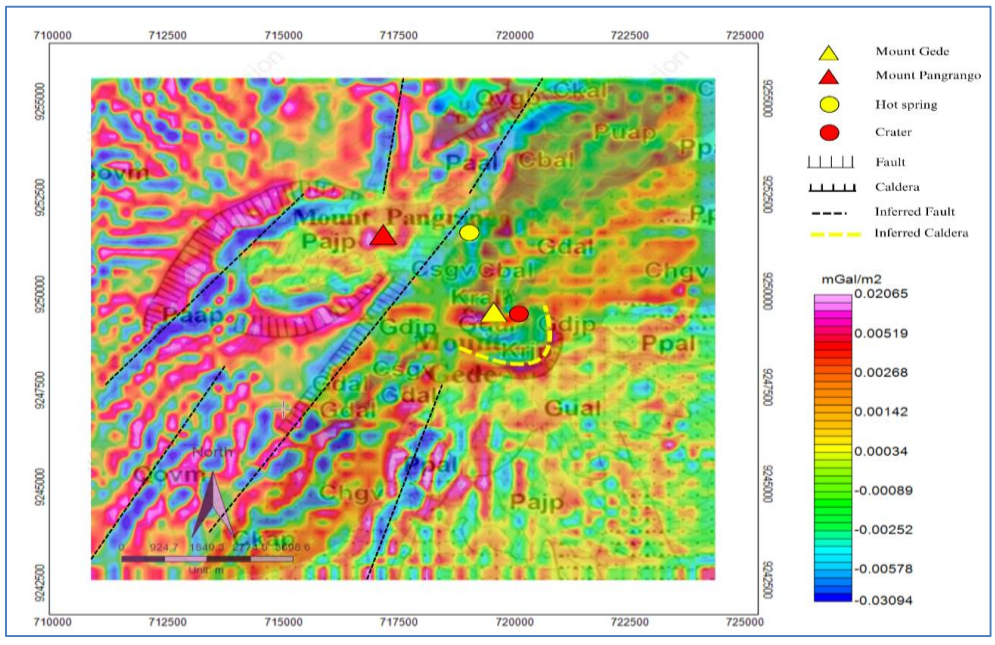

Fig. 9. Vertical derivative representation of Mount Gede-Pangrango Geothermal Prospect area. The results show that zero values are the possible contact zones. The dotted black lines are the inferred faults in the field

(Telford *et al*., 1990). In this study, two types of derivative analysis were applied, first horizontal derivative (FHD) and second vertical derivative (SVD) (Fig. 8 and 9). These analyses aim to identify rock or lithological contact boundaries and subsurface structures based on the residual Bouguer anomaly map.

Second vertical derivative (SVD) analysis was used, with the results shown in Fig. 9. SVD results on a residual contour map, with values ranging from -0.03094 mGal/m^2 to 0.02065 mGal/m^2. The interpretation of the second vertical derivative on the residual anomaly, combined with the regional geological map. The results show that

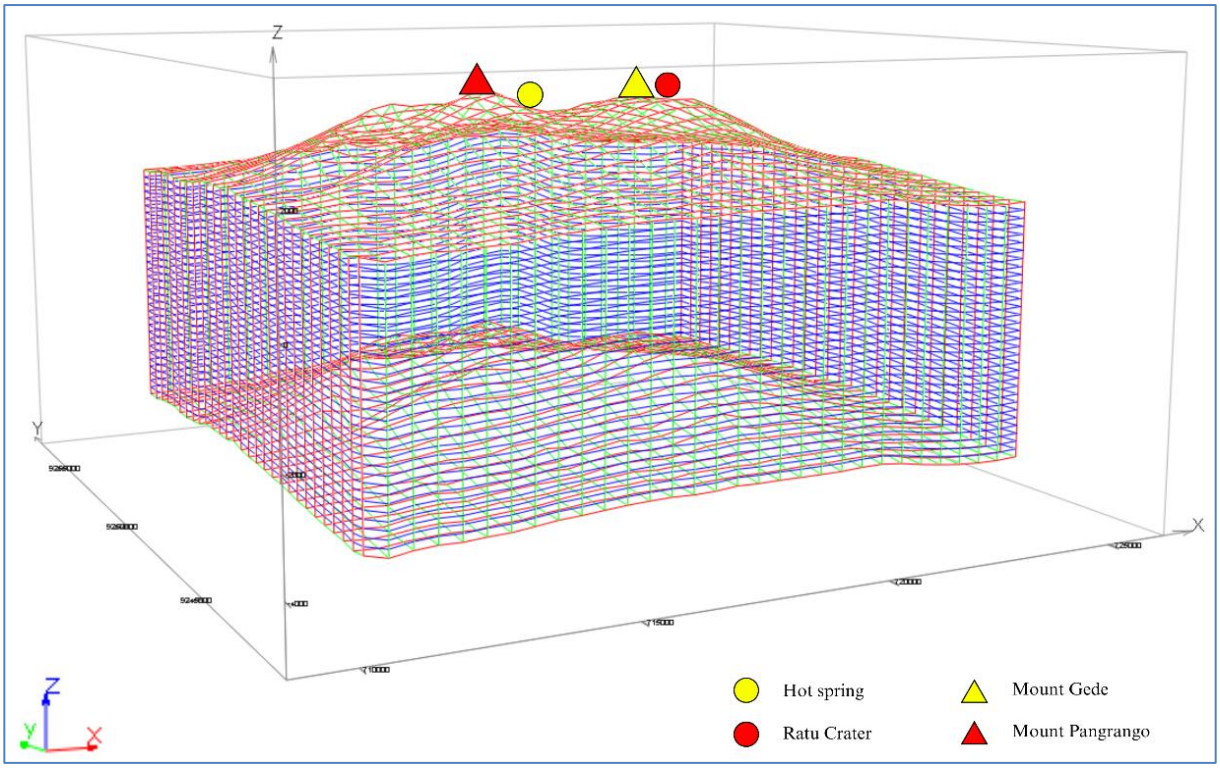

Fig. 10. 3D gravity inversion grid of voxel size 450 m x 450 m x 200 m in the x, y, and z components, respectively. Colored map on top of the model is the Complete Bouguer Anomaly (CBA) with values ranging from 71.94 to 101.69 mGal

zero or minimum values (green colour) represent central points that can be interpreted as lithological boundaries or fault structures (Reynolds, 1997).

The applied filtering methods are unable to describe the density distribution in terms of the shape, volume, and dimensionality of subsurface geological structures. Therefore, 3D inversion modeling is required. The main challenge lies in performing gravity data inversion, which is inherently affected by ambiguity and non-uniqueness of the resulting solution. To minimize these limitations, geological information was integrated so that the inversion modeling results can be validated with greater reliability.

The subsurface of the study area was discretized into 30 × 30 × 30 voxels along the x, y, and z directions. The rectangular cell size was set to 450 m, 450 m, and 200 m in the x, y, and z directions, respectively (Fig. 10). The inversion process involved varying the trade-off regularization parameter to achieve the best fit to the observed data. The model was iteratively refined until the predicted data satisfied the residual chi-squared criterion, yielding the optimal inversion model.

The subsurface density distribution in the study area was then determined using 3D gravity inversion with the VOXI Modeling Tool on the Horin Geophysical Exploration cloud platform, which supports clustered computing to transform potential field data into a 3D model. This voxel-based tool employs the Cartesian cut cell (CCC) method and an iterative reweighting inversion algorithm developed by Ingram *et al*. (2003) and later simplified by Ellis & MacLeod (2013) to produce a more efficient, accurate, and simplified geometric representation of geological surfaces.

The iterative re-weighting least squares (IRLS) algorithm was applied to iteratively solve the optimization problem using weighted least squares calculations. Regularization through the misfit function was implemented to obtain a stable solution of the objective function between observed and calculated values. The degree of agreement between the modeled response and the observed data was assessed using the reduced chi-squared misfit.

3.1. *Discussion*

The gravity method plays a crucial role in geothermal resource exploration as it can detect subsurface density variations associated with geological structures such as faults, fractures, and intrusive bodies. Based

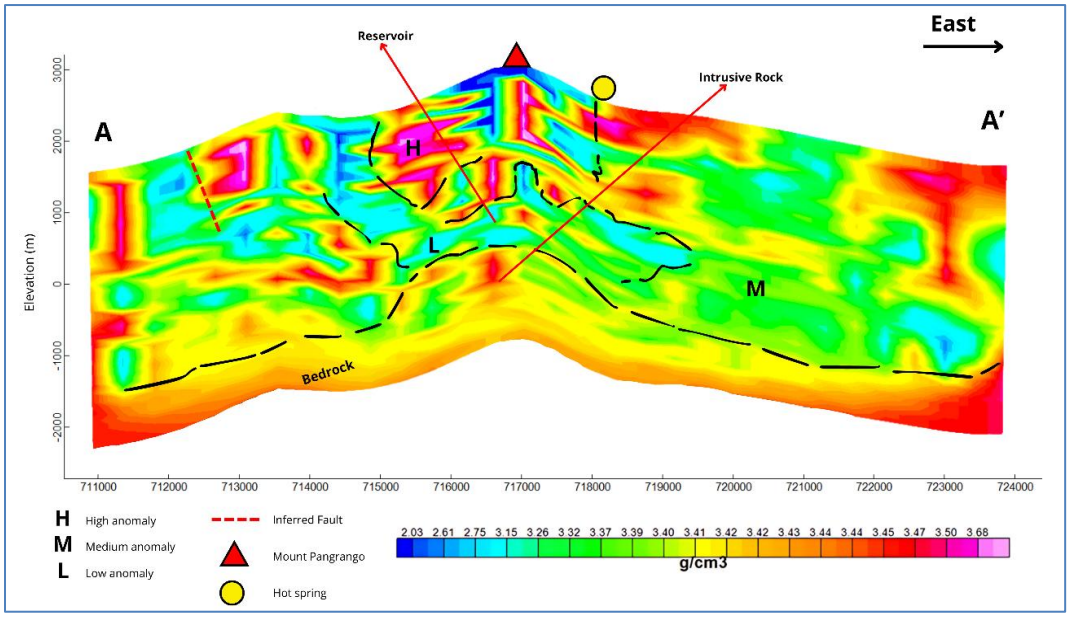

Fig. 11. A-A' Cross-section of the subsurface density in the West-East direction crossing Mount Pangrango and hot springs

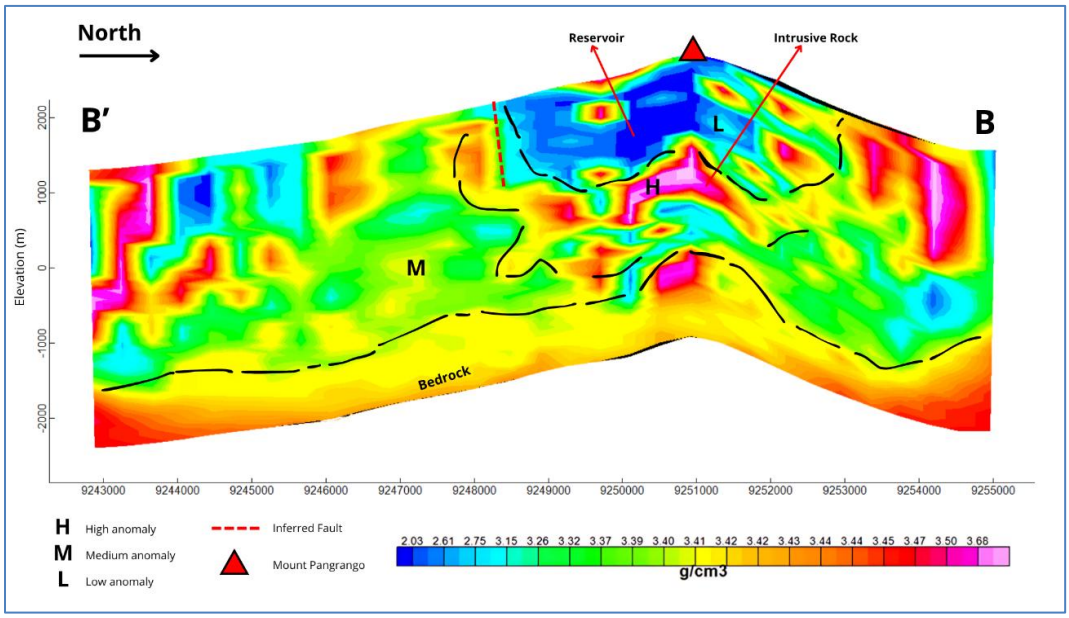

Fig. 12. B-B' cross-section of the subsurface density in the North-South direction crossing Mount Pangrango

on the residual anomaly map (Fig. 7), the Gede–Pangrango geothermal prospect area exhibits three main anomaly zones—high, medium, and low. The high anomaly zones are concentrated around Mount Gede and Mount Pangrango, correlating with volcanic rock formations and fault zones identified in the geological map. These zones are interpreted as dense rock bodies or intrusive formations with high compactness. Conversely, the low anomaly zones are associated with pyroclastic deposits and hydrothermally altered rocks formed by ascending geothermal fluids. The residual anomaly map also reveals contact anomaly zones aligned with NE–SW trending faults separating Mount Gede and Mount Pangrango.

Further analysis using the first horizontal derivative (FHD) and second vertical derivative (SVD) reinforces the

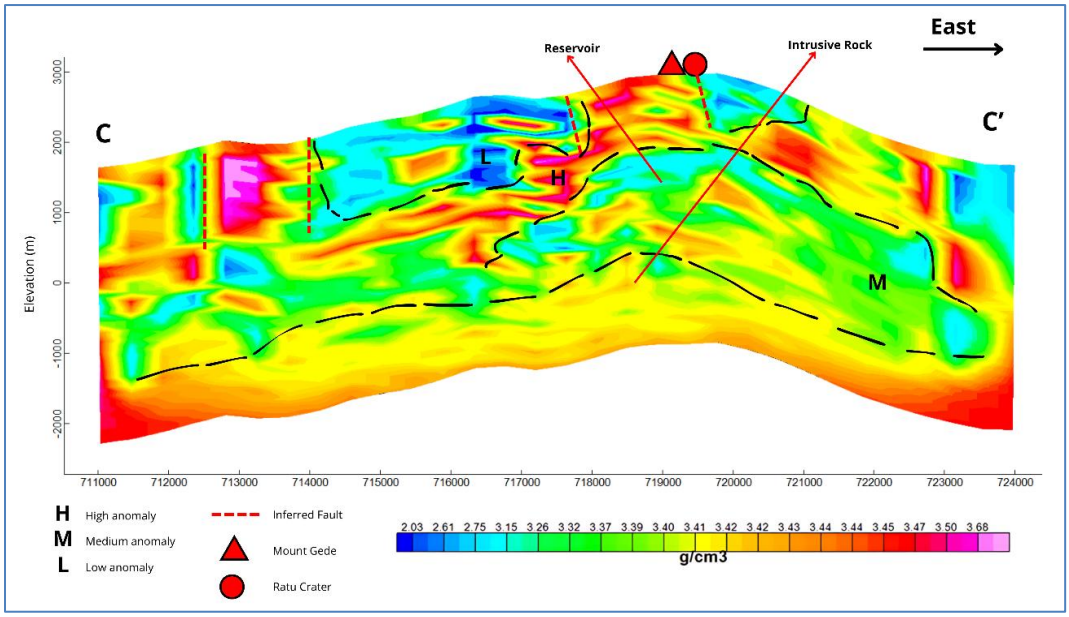

Fig. 13. C-C' cross-section of the subsurface density in the West-East direction crossing Mount Gede and Ratu crater

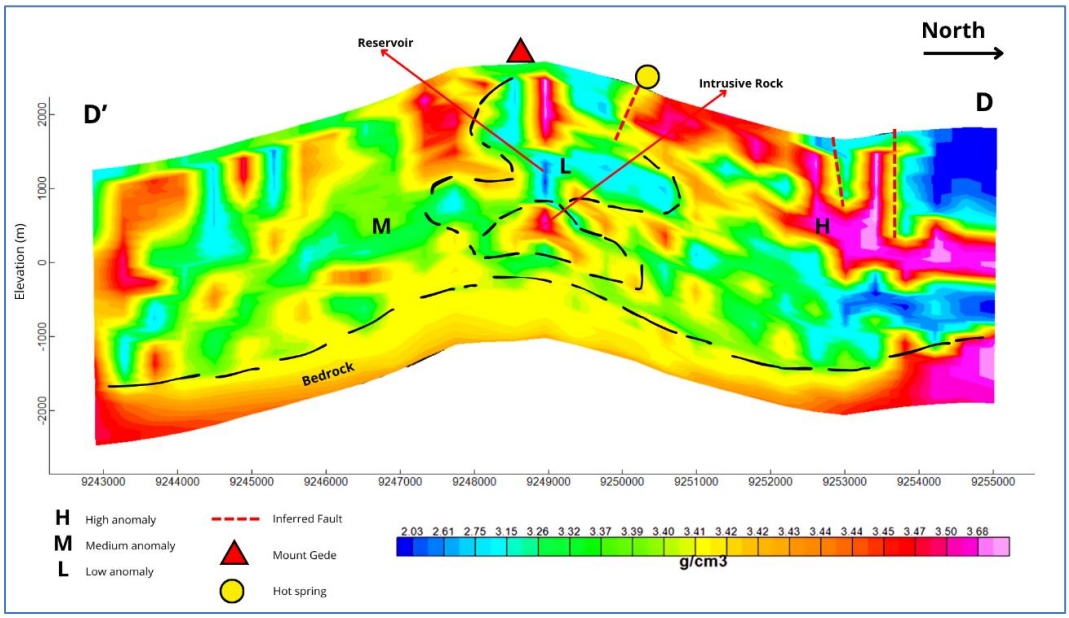

Fig. 14. D-D' cross-section of the subsurface density in the West-East direction crossing Mount Gede and Ratu crater

interpretation derived from the Bouguer anomaly map by highlighting the boundaries of subsurface structures that control the geothermal system. High FHD values indicate areas with significant anomaly contrasts (Fig. 8), while zero values in the SVD correspond to transition zones between rocks with different physical properties, closely related to faults and fractures (Fig. 9). This pattern delineates a dominant northeast–southwest (NE–SW) fault direction, consistent with the geological map, which represents zones of high permeability that allow hydrothermal fluid migration. The correlation among FHD, SVD, and geological data confirms that regional faults act as both primary conduits for geothermal fluid flow and natural boundaries separating dense intrusive rocks from highly porous altered rocks.

Interpretations from the 2D cross-sectional models along lines A–A′, B–B′, C–C′, and D–D′ provide a more

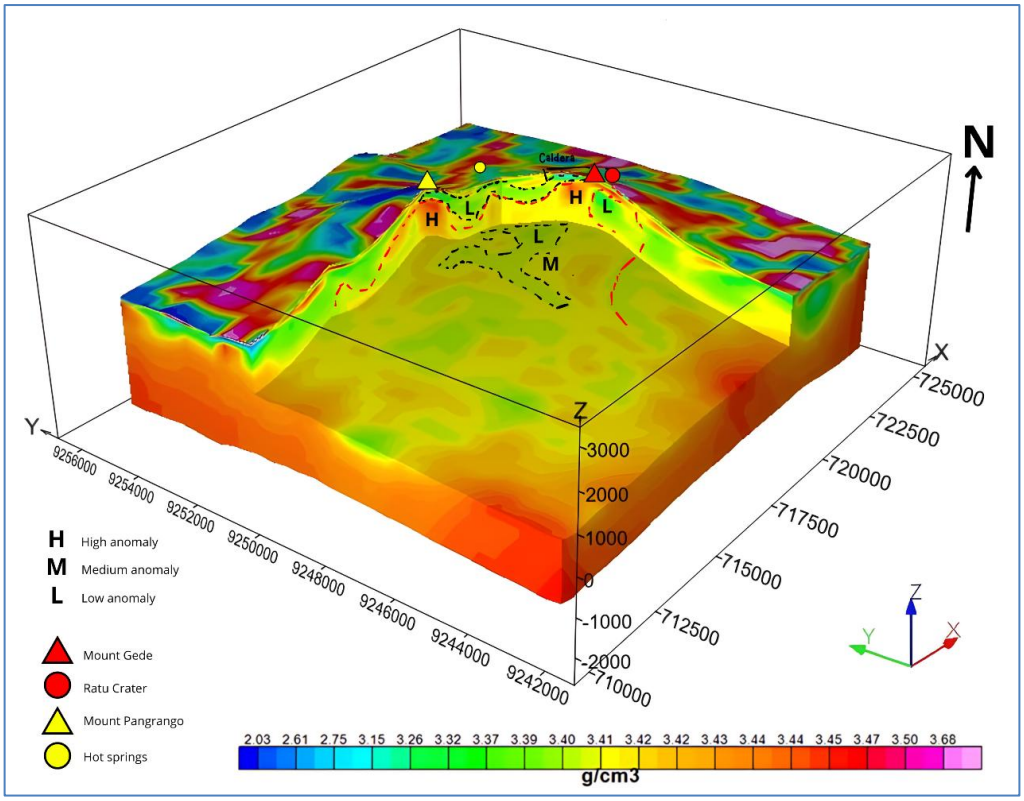

Fig. 15. 3D Modelling Density from Mount Gede-Pangrango Geothermal Prospect Area

detailed understanding of subsurface configuration. The cross-section orientations follow geological slicing lines designed to intersect key structural features such as NE–SW faults, caldera edges, and geothermal manifestation zones. The A–A′ section, crossing Mount Pangrango toward the western hot spring area, reveals a low-density zone (blue to light-green colors) beneath the mountain peak (Fig. 11). This zone is interpreted as hydrothermally altered, fluid-saturated rocks controlled by the NE–SW fault, acting as a geothermal reservoir located at depths of approximately 1–2 km. The B–B′ section (Fig. 12), trending north to south, shows a high-density intrusion (red to pink) interpreted as diorite, basaltic, or andesitic rocks functioning as a heat source for the overlying geothermal system. Above the intrusion lies a low-density layer representing the main geothermal reservoir beneath Mount Pangrango.

In the C–C′ section (Fig. 13), which cuts across Mount Gede and Ratu Crater, lateral heterogeneity is observed, characterized by isolated low-density rocks surrounded by transitional-density zones. This suggests that the geothermal reservoir beneath Mount Gede is non-homogeneous and likely consists of several sub-reservoirs that are partially interconnected. The D–D′ section (Fig. 14), extending across Mount Gede and the eastern hot spring area, exhibits a low-density layer at depths of 1–2 km interpreted as the reservoir, underlain by a dense intrusive body acting as the primary heat source. The overall 2D profiles indicate a close spatial relationship among intrusive rocks, fracture zones, and geothermal fluid systems.

The three-dimensional (3D) density modeling provides a more comprehensive representation of the interconnection between the geothermal systems of Mount Gede and Mount Pangrango (Fig. 15). The model reveals interactions between high- and low-density zones that delineate the relationships among the heat source, cap rock, and reservoir. Low – density zones extend northeastward beneath the volcanic complex and are associated with surface manifestations such as hot springs, while high-density zones near the volcanic centers indicate intrusive bodies serving as heat sources. This spatial pattern suggests a conductive–convective geothermal system, in which hot fluids ascend through fault zones and flow laterally within highly porous altered rock layers.

Overall, the modeling results demonstrate a strong connection between the geothermal systems of Mount Gede and Mount Pangrango. The elongated low-density zone between the two peaks indicates a potential hydraulic

linkage. Fluid circulation likely occurs through major faults acting as both vertical and lateral channels, enabling heat and fluid transfer from the heat source beneath Mount Pangrango to the reservoir beneath Mount Gede, or vice versa. The spatial coherence between low-anomaly zones, active faults, and surface geothermal manifestations supports the interpretation that the Gede–Pangrango volcanic complex operates as an integrated hydrothermal system governed by regional fault structures and ongoing volcanic activity.

4. Conclusions

The gravity modeling results reveal a strong interconnection between the geothermal systems of Mount Gede and Mount Pangrango, highlighting the significance of subsurface density variations in understanding geothermal processes. The integration of residual anomaly, FHD, and SVD analyses successfully delineates the NE–SW fault system that controls the geothermal fluid migration, separating dense intrusive rocks from low-density, hydrothermally altered formations. The 2D and 3D subsurface density models confirm that these faults act as both vertical and lateral conduits for heat and fluid transfer, forming a conductive–convective geothermal system. The elongated low-density zone between Mount Gede and Mount Pangrango indicates potential hydraulic connectivity, where heat and fluids circulate between reservoirs beneath both volcanic centers. Collectively, these findings demonstrate that the Gede–Pangrango geothermal prospect represents an integrated hydrothermal system governed by fault-controlled permeability and active volcanic processes.

Acknowledgment

This work was supported by the *Riset Utama B* research scheme funded by *Selain APBN FSM UNDIP* under the Decree of the Dean of the Faculty of Science and Mathematics, Universitas Diponegoro, Number: 22/UN7.F8/HK/II/2025.

Data availability

Data will be made available on request

Authors' Contributions

Agus Setyawan: Conceptualization, research design, supervision, validation, writing of the original draft, and critical review of the manuscript. *(email: agussetyawan@fisika.fsm.undip.ac.id).*
Putri Permata Hati Suryo Basuki: Data analysis, interpretation of results, literature review, writing of the original draft, and manuscript preparation. *(email: putrisuryoo@alumni.undip.ac.id).*
Ahmad Ali Muckharom: Data acquisition, data processing, methodology development, visualization, formal analysis, and writing of the original draft. *(email: ahmadalimuckharom@gmail.com).*
Tony Yulianto: Methodological guidance, interpretation of geophysical results, validation, and manuscript review. *(email: tonyyulianto@lecturer.undip.ac.id).*
Rahmat Gernowo: Supervision, technical guidance, validation of data processing, and critical revision of the manuscript. *(email: rahmatgernowo@lecturer.undip.ac.id).*
Udi Harmoko: Scientific supervision, interpretation of subsurface/geophysical findings, and manuscript review. *(email: udiharmoko@fisika.fsm.undip.ac.id).*
Muhammad Fahmi: Data support, technical assistance, visualization support, and review of the manuscript. *(email: muhammadfahmi@fisika.fsm.undip.ac.id).*

Disclaimer: The contents and views expressed in this research article are the views of the authors and do not necessarily reflect the views of the organizations they belong to.

References

Agustin, A., 2019, "Geologi Gunung Gede Pangrango: Kajian litologi dan morfologi (in Indonesia)". *Jurnal Ilmiah Geologi*, **12**, 1, 1–10.

Agustine, E., Pranatikta, K. A., Budianto, M. A., Mariyanto, Iriyanti, M., Hapsoro, C. A., & Indriana, R. D., 2023, "Identification of mud volcano's structure using gravity satellite and fault fracture density analysis: a case study Ciuyah mud volcano, Kuningan, West Java". *Sains Malaysiana*, **52**, 11, 3013–3026. https://doi.org/10.17576/jsm-2023-5211-01.

Blakely, R. J., 1995, "Potential theory in gravity and magnetic applications", Cambridge University Press. https://doi.org/https://doi.org/10.1017/CBO9780511549816.

Ellis, R. G., & MacLeod, I. N., 2013, "Constrained voxel inversion using the Cartesian cut cell method". *ASEG Extended Abstracts*, **2013**, 1, 1–4. https://doi.org/10.1071/aseg2013ab222.

Eyike, A., Werner, S. C., Ebbing, J., & Dicoum, E. M., 2010, "On the use of global potential field models for regional interpretation of the West and Central African Rift System". *Tectonophysics*, **492**, 1–4, 25–39. https://doi.org/10.1016/j.tecto.2010.04.026.

Gunawan, B., Anjani, A., & Anjalni, A., 2022, "Identifikasi pemodelan 2D dan suhu permukaan daerah panas bumi Gunung Gede-Pangrango, Jawa Barat menggunakan metode gravitasi (in Indonesia)". *Journal of Engineering Environmental Energy and Science*, **1**, 1, 1–14. https://doi.org/https://doi.org/10.31599/q44a0603.

Hafidh, M. H., Muckharom, A. A., Setyawan, A., & Arianto, F., 2025, "Subsurface modeling using gravity data in the Geureudong volcano geothermal prospect area". *International Journal of Research and Review*, **12**, 6, 261–269. https://doi.org/10.52403/ijrr.20250631.

Haty, I. P., Yudiantoro, D. F., Al Farizzi, M. I., Riyadurrizqy, M. S., Santosa, W. B., & Lukita, A. D., 2023, "Interpretasi

morfostratigrafi berdasarkan citra penginderaan jauh Gunung Gede dan sekitarnya, Jawa Barat, Indonesia (in Indonesia)". *Jurnal Ilmiah Geologi Pangea*, **10,** Special edition 1.

Hinze, W. J., von Frese, R. R. B., & Saad, A. H., 2012, "*Gravity and Magnetic Exploration*", Cambridge University Press. https://doi.org/https://doi.org/10.1017/CBO9780511843129.

Hirt, C., Claessens, S., Fecher, T., Kuhn, M., Pail, R., & Rexer, M., 2013, "New ultrahigh-resolution picture of Earth's gravity field". *Geophysical Research Letters*, **40**, 16, 4279–4283. https://doi.org/10.1002/grl.50838.

Indriana, R. D., Nurwidyanto, M. I., & Widada, S., 2021, "Re-modeling kaligarang fault base on satellite gravity data". *Journal of Physics: Conference Series*, **1943**, 1. https://doi.org/10.1088/1742-6596/1943/1/012004.

Indriana, R. D., Rahmani, I. Q., Setyawan, A., Muckharom, A. A., & Lewerissa, R., 2026, "Integrating Landsat-8, EMAG2v3, and GGMplus gravity data for geothermal prospect zonation at Dormant Volcano (case: Mount Pusuk Buhit, North Sumatra, Indonesia)". *Geographia Technica*, **21**, 70–86. https://doi.org/10.21163/GT_2026.213.05.

Ingram, D. M., Causon, D. M., & Mingham, C. G., 2003, "Developments in Cartesian cut cell methods". *Mathematics and Computers in Simulation*, **61**, 561–572. https://doi.org/10.1016/S0378-4754(02)00107-6.

Iswahyudi, S., 2014, "*Delineasi reservoir sistem hidrotermal Gede - Pangrango berdasarkan data geokimia fluida dan struktur geologi (in Indonesia)*". Institut Teknologi Bandung.

KESDM. (2017). Potensi panas bumi Indonesia (in Indonesia) (Jilid 1). Direktorat Panas Bumi, Direktorat Jenderal Energi Baru, Terbarukan, Konservasi Energi, Kementerian Energi dan Sumber Daya Mineral. https://books.google.co.id/books?id=C9k3yAEACAAJ .

KESDM. (2023, February 15). *Kembangkan infrastruktur energi di Cipanas, Pemerintah utamakan pembangunan ramah lingkungan (in Indonesia)*. Kementerian ESDM. https://www.esdm.go.id/en/media-center/news-archives/ kembangkan-infrastruktur-energi-di-cipanas-pemerintah-utamakan-pembangunan-ramah-lingkungan.

Kusumadinata., 1979, *Data dasar gunung api Indonesia (in Indonesia)*. Directorate of Volcanology.

Lowrie, William., 2007, *Fundamentals of geophysics*. Cambridge University Press. https://doi.org/10.1017/9781108685917.

Muckharom, A. A., Setyawan, A., Rahmani, I. Q., Dwi Indriana, R., & Martha, A. A., 2026, "Geothermal resource assessment on Sumatra Island: Estimating thermal gradient and heat flow based on aeromagnetic data via Curie point analysis". *Journal of Applied Science and Engineering*, **31**, 26031017. https://doi.org/10.6180/jase.202608_31.017.

Muttaqien, I., & Nerjaman, J., 2021, "Two-dimensional inversion modeling of magnetotelluric (MT) synthetic data of a graben structure using SimPEG". *Riset Geologi Dan Pertambangan*, **31**, 1, 1–12. https://doi.org/10.14203/risetgeotam2021.v31.1121.

Parasnis, D. S., & Cook, A. H., 1952, "A study of rock densities in the English Midlands". *Geophysical Journal International*, **6**, 5, 252–271.https://doi.org/https://doi.org/10.1111/j.1365-246X.1952.tb03013.x.

Parasnis, D. Shripad., 1997, *Principles of applied geophysics* (5th ed.). Chapman and Hall. https://books.google.co.id/books?id=yDuI0QEACAAJ.

Phillips, J. D., 2002, "*Processing and interpretation of Aeromagnetic data for the Santa Cruz Basin - Patagonia Mountains Area, South-Central*", *Arizona*. https://doi.org/https://doi.org/10.3133/ofr0298.

Pratiwi, R. N. J., Martha, A. A., Hartono, H., Wijayanti, R., Muckharom, A. A., Kinanti, A. S. A., & Ngaeni, N. P. N., 2026, "Identification of Subsurface Geological Structures of the Arjuno-Welirang Geothermal Potential Area Using the Gravity Method". *Malaysian Journal of Fundamental and Applied Sciences*, **22**, 1, 90–101. https://doi.org/10.11113/mjfas.v22n1.4573.

Prihatini, A., Indriana, R. D., Setyawan, A., & Fahmi, M., 2025, "Seismotectonic characteristics of the Cugenang Fault, Cianjur, West Java, based on a-Value, b-Value, seismic moment and satellite gravity (Earthquake data of 2008-2023)". *Sains Malaysiana*, **54**, 8, 1889–1900. https://doi.org/10.17576/jsm-2025-5408-02.

Reynolds, J. M., 1997, "*An introduction to applied and environmental geophysics*" (2nd ed.). John Wiley & Sons. https://books.google.co.id/books?id=hzC_7CIirdYC .

Sarkowi, M., 2014, *Eksplorasi gaya berat (in Indonesia)*. Graha Ilmu.

Saxena, S. Kumar., & Candela, P. A., 1986, "*Chemistry and physics of terrestrial planets*", *Springer Verlag*. https://doi.org/10.1007/978-1-4612-4928-3.

Setyawan, A., Nadhila, M. F., Suseno, J. E., & Indriana, R. D., 2024, "2D sparse inversion gravity method for subsurface interpretation by Simpeg: A case study of Ungaran Volcano". *Journal of Southwest Jiaotong University*, **59**, 3. https://doi.org/10.35741/issn.0258-2724.59.3.36.

Setyawan, A., Yudianto, H., Nishijima, J., & Hakim, S., 2015, "Horizontal gradient analysis for gravity and magnetic data beneath Gedongsongo geothermal manifestations, Ungaran, Indonesia". *Proceedings World Geothermal Congress*, 19–25.

Situmorang, & Hadisantono, R., 1992, "*Peta geologi Gunungapi Gede, Cianjur, Jawa Barat (in Indonesia)*. https://geologi.esdm.go.id/storage/publikasi/GXapQy1MEQRwTlqVpOyXyJ1DXWdz4ycNZFrnNJhd.pdf.

Tatham, R. H., 2011, "*An Introduction to Geophysical Exploration: Third Edition* (3rd ed.). *Eos, Transactions American Geophysical Union*. **84**, https://doi.org/10.1029/2003EO120005.

Telford, W., Geldart, L., & Sheriff, R., 1990, *Applied Geophysics* (2nd ed.). Cambridge University Press. https://doi.org/10.1017/CBO9781139167932.

Yasmin, H. S., Pirzada, S. J., Sahroni, T. R., Soekarno, H., Pranoto, B., Puspa, A. D., & Alfisah., 2024, "2D Geological Structure Identification in Mount Ciremai Geothermal Area using the GGMplus Data". *IOP Conference Series: Earth and Environmental Science*, **1344**, 1. https://doi.org/10.1088/1755-1315/1344/1/012017.